PROCEEDINGS. "Twenty-Seventh Workshop on Geothermal Reservoir Engineering
Stanford University, Stanford, California, January 28-30, 2002
SGP-TR-171

DECLINE CURVE ANALYSIS FOR NATURALLY FRACTURED RESERVOIRS WITH TRANSIENT INTERPOROSITY FLOW

Héctor Pulido B. [1,2], Fernando Samaniego V.[2], Jesús Rivera R.[2] , Rodolfo Camacho V.[1,2] and César Suárez A.[3]
1. PEMEX; 2. National University of Mexico; 3. Michoacán University.

ABSTRACT

Constant producing pressure solutions that define declining production rates with time, for a naturally fractured reservoir, with transient interporosity flow are presented. The solutions for the dimensionless flow rate are based on a model presented by Cinco-Ley, Samaniego and Kucuk. In this work the model was extended to include constant producing pressure in both infinite and finite systems. The results obtained for a finite no flow outer boundary are new and surprising. Similarly to Da Prat et al.[1], it was found that the flow rate for conditions of fracture skin greater than 10, shows initially rapid decline, becomes nearly constant for a period, and then a final decline in rate takes place.

The same criterion established by Da Prat et al.[1] for the estimation of the outer radius of a reservoir, r_e , requiring that the almost constant flow rate period be reached by the data is applicable to the present transient interporosity flow model. However, the estimation of r_e from this method is higher for fixed values of the ω and λ parameters. A field example is presented to illustrate the method of type curve matching for a naturally fractured reservoir with transient interporosity flow.

The values of ω and λ are determined from the best match and this is particularly important for the case of production forecasting by numerical simulation. The results show that the initial decline could be a key factor in deciding whether to complete or abandon a well, and for a practical viewpoint, given an initial value for the flow rate, it is important to know the time required to deplete the two porosity system.

INTRODUCTION

Naturally Fractured Reservoirs (NFR) consist of heterogeneous porous media where the openings (fissures and fractures) vary considerably in size. Fractures and openings of large size generate vugs and interconnected channels, whereas the fine cracks form block systems which are the main body of the reservoir.

In the past, the analysis of short time flow rate data to obtain reservoirs parameters was not a common technique, mainly due to the difficulties in obtaining accurate measurements of the flow rate as compared to high resolution pressure measurements. However, the advent of new production tools, like the real time flow meter (see Kucuk and Ayestaran[2], Stewart et al.[3]), has made possible the analysis of simultaneously measured pressures and flow rates in a transient well test. The advantage of incorporating the measured flow rate, is that the type curve matching technique is improved, giving more information regarding the uniqueness as to the type of reservoir being dealt with, i.e., fractured, multi layer, composite, etc. In a fractured formation we may have wells initially producing at a high rate where in some cases, production starts to decline after a few hours without any clear explanation. Therefore, analyzing the transient flow rate behavior in a well completed in a fractured formation will add more information that will result in a more complete evaluation analysis. From an engineering and economic viewpoint, the initial decline could be a key factor in deciding whether to complete or abandon a well.

NFR have been studied extensively in the petroleum literature. One of the first such studies was published by Pirson[4] in 1953. Pollard[5] presented one of the first pressure models available for interpretation of well test data; however, the graphical technique proposed is susceptible to error caused by approximations in the mathematical model.

The first to present a detailed discussion of the transient radial flow of a slightly compressible fluid through a naturally fractured reservoir were Barenblatt and Zheltov[6] and Barenblatt et al.[7]; these authors assume that the flow occurs only in the fracture medium and that the matrix blocks are a source that delivers flow to the fracture system and that this flow could be considered under pseudosteady state flow conditions. Warren and Root[8] obtained analytical solutions useful for well test analysis found that data in NFR by using the formulation of Barenblatt et al.; they for a pressure test show two parallel semilog straight lines, whose slope is related to the flow capacity of the formation. These theoretical results were supported later by two field examples presented by the same authors[9]; this model is considered the forerunner of modern interpretation of two porosity systems.

Odeh[10] presented a model also assuming pseudosteady state flow conditions in the matrix and concluded that a fractured system behaves like a homogeneous one. Later, Adams et al.[11] presented field examples of pressure test of a fractured reservoir, and used a radial discontinuity model as an interpretation tool. The field data exhibited two straight line portions, such that the first had a slope twice the slope of the second. Kazemi[12] was first to consider transient matrix flow in a numerical radial model

assuming the NFR made up of horizontal fractures interbeded with matrix strata; his results are similar to those of Warren and Root, with the exception of a smooth unsteady state transition behavior in between the two semilog straight lines, compared to the pseudo-steady state zone of Warren and Root model.
Gringarten and Witherspoon[13] reviewed the theory on transient pressure analysis for both hydraulically and NFR. Later de Swaan[14] presented analytical transient solutions for a well producing at constant rate; his model exclusively involves flow properties and dimensions of the fracture and the matrix systems and introduced new diffusivity definitions useful for reservoir characterization.

Crawford et al.[15] presented some of the best field examples of pressure transient tests on NFR, concluding that a test properly conducted can be interpreted by the Warren and Root model and indicated that ω and λ should be obtained from field performance. Strobel et al.[16] presented another remarkable field behavior example of a naturally fractured gas reservoir, demonstrating that both fracture permeability and fracture porosity can be estimated from type curve analysis of pressure buildup, interference and pulse tests. Mavor and Cinco-Ley[17] presented solutions for wellbore storage and well damaged conditions for a NFR; they used the pseudosteady state matrix flow condition, and also considered production, both at constant rate and at constant pressure. However, little information is presented concerning the effect of the size of the system on pressure buildup behavior.

Streltsova[18] presented a complete review on the work done on the behavior of NFR. Najurieta[19] further advanced the de Swaan´s model by presenting an approximate solution, showing that pressure behavior can be fully described by five basic parameters. Kucuk and Sawyer[20] described a comprehensive model for gas flow in a NFR; they considered transient flow in both cylindrical and spherical matrix blocks. Gringarten[21] discussed the interpretation of pressure data and clearly showed the relationship among the parameters used in different models. Da Prat et al.[22] have discussed the application of the Muskat method to NFR to calculate the permeability-thickness product.

A remarkable work done on the analysis of pressure data for NFR under practical conditions (influenced by wellbore storage and skin), has been presented by Bourdet and Gringarten[23], Gringarten et al.[24], and Gringarten[25]. They discussed the use of a new type curve for both identification of the flow periods and estimation of parameters. Although the use of the pseudosteady state matrix flow model was recommended, these authors where the first to identify the semilog straight line during the transition period for the transient state matrix-fracture flow conditions; however, no application of this feature was discussed.
Cinco-Ley and Samaniego[26] considered transient interporosity flow and included wellbore storage and skin effect; the matrix fracture transfer was presented in a convolution form which permits the use of different matrix blocks geometries. Streltsova[27] and Serra et al. [28] have presented detailed studies on the pressure behavior of NFR; both papers thoroughly treat the transition period commented on the previously published papers, showing again that during this flow period a semilog plot of p_{wD} vs. t_D exhibits a straight line of slope 0.5756.
Chen et al.[29] presented a model with transient state matrix-fracture flow conditions using linear flow in the matrix for bounded NFR. Moench and Ogata[30], discussed the consideration of the skin in the fractures in NFR. Cinco-Ley, Samaniego and Kucuk[31] presented a model with transient interporosity flow, that considers multiple matrix block size and matrix-fracture flow restriction (*fracture skin* in this work), for a well producing at constant rate, with wellbore storage and skin in an infinite system; the model that considers only one matrix block size without fracture skin is the same model of Cinco-Ley and Samaniego[26]. With this model is possible to generate the pseudosteady interporosity flow using a big enough matrix-fracture flow restriction.

Although decline curve analysis is widely used, specific methods for NFR with transient interporosity flow are not available. It is the objective of this paper to develop a model with the above characteristics to study decline curve analysis for a NFR. The Cinco-Ley, Samaniego and Kucuk model[31] was chosen as the basis for this work due to its consideration of transient interporosity flow, with multiple size, matrix block and matrix-fracture flow restriction. In this study the model was extended using constant producing pressure in both infinite and finite systems, with only one matrix block size and new approximate analytical solutions are presented for small and long times.

Partial Differential Equation

The fundamental partial differential equation is:
Radial flow in the fractures

$$\frac{\partial^2 p_{fD}(r_D,t_D)}{\partial r_D^2}+\frac{1}{r_D}\frac{\partial p_{fD}(r_D,t_D)}{\partial r_D}-[1-\omega]\ C_{fbD}\frac{\partial p_{fD}(r_D,t_D)}{\partial t_D}*F(\eta_{mD},t_D)=$$
$$=\omega\frac{\partial\ p_{fD}(r_D,t_D)}{\partial\ t_D} \qquad (1)$$

Initial condition: $p_{fD}(r_D,0)=0$ (2)

Internal boundary: constant pressure and skin.

$$p_{fD}(1,t_D)-S_w\frac{\partial p_{fD}(1,t_D)}{\partial r_D}=1 \qquad (3)$$

External boundary: infinite reservoir.

$$\lim_{r_D\to\infty} p_{fD}(r_D,t_D)=0 \qquad (4)$$

Or closed reservoir

$$\frac{\partial p_{fD}(r_{eD}, t_D)}{\partial r_D} = 0 \qquad (5)$$

The matrix to fracture flow functions are given as:
For strata:

$$F(\eta_{mD}, t_D) = 4\eta_{mD} \sum_{n=0}^{\infty} e^{-\eta_{mD}(2n+1)^2 \pi^2 t_D} \qquad (6)$$

For spheres:

$$F(\eta_{mD}, t_D) = 4\eta_{mD} \sum_{n=1}^{\infty} e^{-4\eta_{mD} n^2 \pi^2 t_D} \qquad (7)$$

The dimensionless flow rate into the wellbore is given by:

$$q_D(t_D) = \frac{-\partial p_{fD}(1, t_D)}{\partial r_D} \qquad (8)$$

The cumulative production is related to the flow rate by:

$$N_{pD}(t_D) = \int_0^{t_D} q_D(t_D')dt_D' \qquad (9)$$

where the dimensionless variables are defined as follows:

$$r_D = \frac{r}{r_w}; \quad r_{eD} = \frac{r_e}{r_w}; \quad t_D = \frac{2.637\ x10^{-4} k_{fb} t}{[\phi_m c_{tm} + \phi_{fb} c_{tf}]\mu r_w^2};$$

$$r_w' = r_w e^{-S_w}; \quad r_{eD}' = \frac{r_e}{r_w'}; \quad p_{fD}(r_D, t_D) = \frac{p_i - p_f(r,t)}{p_i - p_{wf}};$$

$$p_{wD}(t_D) = \frac{p_i - p(r_w, t)}{p_i - p_{wf}}; \quad q_D(t_D) = \frac{141.2\mu B q(t)}{k_{fb} h[p_i - p_{wf}]};$$

$$\omega = \frac{\phi_{fb} c_{tf}}{\phi_{fb} c_{tf} + \phi_{mb} c_{tm}} = \frac{\phi_{fb} c_{tf}}{(\phi c_t)_t}; \quad \lambda = \frac{4n[n+2] k_m r_w^2}{\varsigma^2 k_{fb}};$$

$$\eta_{mD} = \frac{\eta_m r_w^2}{\eta_{fb} \varsigma^2} = \frac{k_m (\phi c_t)_t r_w^2}{k_{fb} (\phi c_t)_m \varsigma^2} = \frac{(\phi c_t)_t \lambda}{4n[n+2](\phi c_t)_m} = \frac{V_m}{4n[n+2]V_b} \frac{\lambda}{[1-\omega]}$$

$$t_D' = \frac{t_D}{\omega} = \frac{k_{fb} t}{\phi_{fb} \mu c_{tf} r_w^2}; \quad C_{fb} = \frac{A_{surf}}{V_b} = \frac{A_{surf}}{V_m + V_f};$$

$$C_{fbD} = \frac{C_{fb} V_b \varsigma}{V_m}; \quad \lambda = \frac{C_{fbD}}{S_f} \eta_{mD}; \quad r_{DH} = \frac{r_{esf}}{r_w}; \quad z_{DH} = \frac{H}{r_w}$$

For strata: $\varsigma = H$ and for spheres: $\varsigma = r_{esf}$

$$S_f = \frac{k_m x_d}{k_d \varsigma}$$

Method of Solution

A common method for solving a flow equation under the conditions given is to use the Laplace transformation. The advantages of this method have been described by van Everdingen and Hurst[32]. The equations are transformed into a system of ordinary differential equations which can be solved analytically. The resulting solution in the transformed space is a function of the Laplace parameter and the radius. To obtain the solution in real time, the inverse Laplace transform is used. In our work, the inverse was found using the Stehfest[33] algorithm this approach was introduced in the reservoir flow studies by Ramey, and used has been successfully by many authors. Included in this work is a short and long time analysis, which provides simple expressions in real time; these expressions can be used to verify results obtained from the numerical algorithm, as well as to select the adequate N parameter (equal to 10 for the present study) to be used to perform the numerical inversion, in addition to being useful in interpretation of results. The analytical solutions in Laplace space for both the infinite and the closed outer boundaries are given in the following sections.

Infinite outer boundary

The transient solution obtained in this work for the dimensionless flow rate is given by:

$$\overline{q}_D(s) = \frac{\sqrt{sf(s)}K_1(\sqrt{sf(s)})}{s[K_0(\sqrt{sf(s)}) + S_w\sqrt{sf(s)}K_1(\sqrt{sf(s)})]} \qquad (10)$$

where the transfer function is:

$$f(s) = \omega + [1-\omega]C_{fbD}\overline{F}(\eta_{mD}, s)/(1 + 4S_f\overline{F}(\eta_{mD}, s)) \qquad (11)$$

For strata:

$$\overline{F}(\eta_{mD}, s) = \frac{1}{4\sqrt{s/\eta_{mD}}} \tanh\left(\sqrt{s/\eta_{mD}}/2\right) \qquad (12)$$

and for spheres:

$$\overline{F}(\eta_{mD}, s) = \frac{1}{4\sqrt{s/\eta_{mD}}}\left[\coth\left(\sqrt{s/\eta_{mD}}/2\right) - \frac{2}{\sqrt{s/\eta_{mD}}}\right] \qquad (13)$$

For small times, a solution to Eq. 10 can be obtained substituting the modified Bessel functions by their asymptotic expansions. The dimensionless flow rate can be expressed:

$$q_D(t_D) = \sqrt{\omega}\left[1 - e^{-t_D/(S_w\sqrt{\omega})}\right] \qquad (14)$$

for $S_w = 0$:

$$q_D(t_D) = \frac{1}{\sqrt{\pi}}\left(\frac{t_D}{\omega}\right)^{-1/2} \qquad (15)$$

In terms of cumulative production:

$$N_{pD}(t_D) = \sqrt{\omega}\left[t_D + S_w\sqrt{\omega}e^{-t_D/(S_w\sqrt{\omega})}\right] \qquad (16)$$

For $S_w = 0$:

$$N_{pD}(t_D) = \frac{2}{\sqrt{\pi}}(\omega t_D)^{1/2} \qquad (17)$$

For conditions of ω =1 and small times, Eq. 17 is identical to that presented by van Everdingen and Hurst[32]. As previously stated the expression obtained for the flow rate can be associated with a homogeneous reservoir through an effective time, $t_D' = t_D/\omega$. Thus, initial production from a NFR in an infinite medium does not detect the presence of the matrix porosity; it behaves like a homogeneous reservoir.

For long times the solution depends the matrix-fracture surface exposed to flow; it can be derived by making a long time approximation for the general solution expressed by Eq. 10; the solution obtained in this work is given by:

$$q_D(t_D) = \frac{2}{\ln\left(\frac{t_D}{\omega + [1-\omega]C_{fbD}/8}\right) + 0.809071 + 2S_w} \quad (18)$$

If ω =1 and $S_w = 0$, the solution reduces to that previously reported by Jacob and Lohman[34]:

$$q_D(t_D) = \frac{2}{\ln(t_D) + 0.80907} \quad (19)$$

The results obtained through transient interporosity flow model, without fracture skin, two values of ω and four values of λ, does not show *constant flow* rate period and give more production that the case with pseudosteady-state transfer. Also, at long times, the solution approaches that for the homogeneous case, as shown in **Fig. 1.**

To generate the pseudo-steady-state flow solution the transient interporosity flow model is used with a value of fracture skin = 6, two values of ω and five values of λ. It can be observed that the bigger λ, the sooner starts the transition flow, as shown in **Fig. 2.**

The same analysis to that of Da Prat et. al., for a non communicating matrix, λ=0, was done. Fig. 3 presents several curves as function of ω, at all times the solution depends on $t_D' = t_D / \omega$.

To generate the pseudo-steady-state flow solution the model with transient interporosity flow is used with a fracture skin = 6 and a non communicating matrix, λ=0, as shown in **Fig. 4.** The ranges used are: $2 \le C_{fbD} \le 6$ and $0 \le S_f \le 10$.

Closed outer boundary

Fetkovitch[35] discussed the findings of Tsarevich and Kuranov[36], regarding that the exponential decline is a long time solution of the constant pressure case. The solution obtained in this work for the dimensionless flow rate, in the Laplace space is given by:

$$\bar{q}_D(s) = \frac{\sqrt{sf(s)}\left[I_1\left(r_{eD}\sqrt{sf(s)}\right)K_1\left(\sqrt{sf(s)}\right) - K_1\left(r_{eD}\sqrt{sf(s)}\right)I_1\left(\sqrt{sf(s)}\right)\right]}{s\left[D_1 - S_w\sqrt{sf(s)}D_2\right]} \quad (20)$$

where:

$$D_1 = K_1\left(r_{eD}\sqrt{sf(s)}\right)I_0\left(\sqrt{sf(s)}\right) + I_0\left(r_{eD}\sqrt{sf(s)}\right)K_0\left(\sqrt{sf(s)}\right) \quad (21)$$

$$D_2 = K_1\left(r_{eD}\sqrt{sf(s)}\right)I_1\left(\sqrt{sf(s)}\right) - I_1\left(r_{eD}\sqrt{sf(s)}\right)K_1\left(\sqrt{sf(s)}\right) \quad (22)$$

and f(s) is defined by Eq. 11.

For short times, as for the homogeneous system, there is no dependence on drainage radius, which means that the system behaves as an infinite medium.

For intermediate times, the value of the flow rate (during the almost constant rate period) depends *strongly* on C_{fbD}, S_f, η_{mD} and ω.

For long times, the flow rate given by Eq. 20 can be expressed in terms of time as:

$$q_D(t_D) = \frac{\left[r_{eD}^2 - 1\right]}{2}\frac{C_{fbD}\,\eta_{mD}}{S_f}e^{-\frac{C_{fbD}\,\eta_{mD}\,t_D}{S_f[1-\omega]}} \quad (23)$$

And for the cumulative production:

$$N_{PD}(t_D) = \frac{r_{eD}^2 - 1}{2}[\omega - 1]\left[e^{-\frac{C_{fbD}\,\eta_{mD}\,t_D}{S_f\,1-\omega}} - 1\right] \quad (24)$$

At long times, for a homogeneous reservoir an exponential decline can be observed for the constant producing pressure case. Thus, results for homogeneous systems can be extended to fractured reservoirs. It can be concluded that, as previously stated in a fractured reservoir, the final decline takes place later in time as compared to the homogeneous case (ω=1). This implies that, it takes longer time to deplete a fractured system.

Eq. 23 should represent the homogeneous solution when either ω = 1 or η_{mD} tends to infinite.

Taking limits in Eq. 23 yields (using L´hopital rule´s):

$$\lim_{\substack{\lambda\to\infty \\ \omega\to 1}} q_D(t_D) = \lim_{\substack{\lambda\to\infty \\ \omega\to 1}}\left[\frac{r_{eD}^2 - 1}{2}\right]\lambda e^{-\frac{\lambda t_D}{1-\omega}} = 0 \quad (25)$$

At long times, for a homogeneous system, the flow rate becomes zero.

At long times ($t_D \to \infty$), from Eq. 24, the cumulative production for a NFR is given by:

$$N_{PD} = \frac{r_{eD}^2 - 1}{2}[1-\omega] \quad (26)$$

The long time solution can be used to explain the observed period of constant flow rate; q_D.

As time increases, the exponential term in Eq. 23 begins to dominate until the flow rate becomes zero.

The series expansion for the exponential is given as follows:

$$e^{-x} = 1 - x + \frac{x^2}{2!} - \frac{x^3}{3!}\ldots$$

For small argument:

$$\frac{C_{fbD}\,\eta_{mD}\,t_D}{S_f[1-\omega]} < 0.01 \quad (27)$$

then $e^{-\frac{C_{fbD}\,\eta_{mD}\,t_D}{S_f[1-\omega]}} \approx 1$, requiring that:

$$t_D < \frac{[1-\omega]S_f}{100\,C_{fbD}\,\eta_{mD}} \quad (28)$$

From both practical and economic point of view, given an initial value for the flow rate, it is important to know how long it takes to completely deplete the fractured reservoir, the flow rate starts to decline when it reaches the approximate value of the flow rate given by Eq. 23, which can be expressed as:

$$q_D(t_D) = \frac{\left[r_{eD}^2 - 1\right]}{2}\frac{C_{fbD}\,\eta_{mD}}{S_f} \quad (29)$$

Results obtained with the model with transient interporosity flow, without fracture skin, for two values

of ω, five values of λ and r_{eD}=50 are presented in Fig. 5. It is shown that for the flow rate first shows a rapid decline, and then it presents a *linear behavior for a long period (the almost constant flow rate period is not shown) and is longer for smaller* λ, after which a final rate decline takes place, as well as at long times the solution is dominated by boundary effects.

It can be noticed from a comparison of Fig. 5 that the cumulative production for the case of transient matrix-fracture flow is higher than for the pseudo-steady state case.

However, when using ***transient interporosity flow with fracture skin***= 6 (given two values of ω and five values of λ), the results are surprising: the flow rate at first shows a rapid decline and then the behavior becomes almost constant for a long period (*equivalent to pseudo-stationary flow)*, after which a final rate decline takes place and shows that the bigger λ, the sooner the transition flow starts, as shown in **Fig. 6**.

Thus, compared to the homogeneous case (ω =1), a longer time is required to deplete a two porosity system.

The analysis similar to Da Prat et. al., for a non communicating matrix, λ=0, where several curves are shown as a function of ω, in all times the solution depends on $t_D' = t_D / \omega$, is presented in **Fig. 7.**

As previously stated, to generate the pseudo-steady flow was the transient interporosity model with fracture skin = 6 conditions for the specific case of a non communicating matrix, λ=0, the solutions, are shown in **Fig. 8.**

Production forecast analysis

For the observed decline in flow rate from an engineering and economic point of view; the initial decline could be a key factor in the completion or abandonment of a well.

Decisions concerning production forecast and estimates of the size of fractured reservoirs should not be based only on the observed initial decline. Ignoring the presence of a fractured system can lead to a great error on the estimation of the cumulative production.

Let us start the analysis of the initial decline by considering the simplest case of a non communicating matrix, λ = 0. In this case, the behavior is the same as that for a homogeneous system, but with $t_D' = t_D / \omega$.

Figs. 7 and **8** show the dimensionless flow rate behavior, in terms of q_D vs. t_D for different values of ω, for values of the fracture skin 0 and 6, respectively. All curves show a defined decline as the final depletion state approaches. An expression for the flow rate can be derived from the dimensionless wellbore pressure function for constant rate production after the onset of pseudo steady state.

van Everdingen and Hurst[32] showed that knowing the pressure in the well, it is possible to find the flow rate by applying the inverse Laplace transformation to the following relationship:

$$\overline{q_D}(s) = \frac{1}{s^2 \overline{p_{wD}}(s)} \qquad (30)$$

Mavor and Cinco-Ley[18] showed that for a closed, bounded two porosity system with pseudo steady state matrix to fracture flow system, p_{wD} at constant rate is given by:

$$p_{wD}(t_D) = \frac{2\pi t_D}{r_{eD}^2 \omega} + \ln(r_{eD}) - 3/4 \qquad (31)$$

Applying the Laplace Transform to the wellbore pressure:

$$\overline{p_{wD}}(s) = \frac{2\pi}{r_{eD}^2 \omega s^2} + \frac{1}{s}\left[\ln(r_{eD}) - 3/4\right] \qquad (32)$$

Substituting Eq. 32 in Eq. 30:

$$\overline{q_D}(s) = \frac{1}{\ln(r_{eD}) - 3/4} \frac{1}{\frac{2\pi}{r_{eD}^2 \omega\left[\ln(r_{eD}) - 3/4\right]} + s} \qquad (33)$$

Inverting to real time:

$$q_D(t_D) = \frac{1}{\ln(r_{eD}) - 3/4} e^{\frac{-2\pi t_D}{r_{eD}^2 \omega\left[\ln(r_{eD}) - 3/4\right]}} \qquad (34)$$

In the case of a non communicating matrix, the initial decline is exponential in nature, and can be described by Eq. 34. Also included in the work of Mavor and Cinco-Ley are the evaluation of parameters λ and ω from decline curves and a study of the observed initial decline in production rate. A procedure for using log-log type curve matching to analyze rate-time data is presented. From the match point, the fracture permeability, ω η_{mD}, r_{eD} and S_w can be calculated. This methodology is easy to apply for well data.

Decline curve analysis using type curves

Fetkovich[35] described a procedure for using log-log type curve matching to analyze rate-time data for a homogeneous system. The same method can be applied to naturally fractured reservoirs as pointed out by Da Prat et al.[23] and Sageev et al[37]. However, the relationship between q_D vs. t_D is controlled by ω and η_{mD}, as well as by C_{fbD}, S_w, S_f; we present a method where ω and η_{mD} can be obtained using only flow rate transient data; the production decline procedure presented for log-log type-curve matching should be simple if ω and η_{mD} can be obtained independently from pressure build up analysis, if this information is not available, it may be necessary to use several type curves to obtain the best match. In this case, for a given r_{eD}, it would be necessary to consider several 3 or 4 values of ω and 4 or 5 values of λ for each ω. As a result, many pairs of ω and λ might be found for a known

r_{eD}. If ω and λ can be obtained from pressure build-up analysis, the particular type-curve to be used in production calculations or matching for estimation of reservoir size can be properly defined.

The solution for homogeneous system may be obtained by setting ω = 1, and it is shown in the figures for comparison with results for a fractured systems. The homogeneous system case is the same solution as that presented by Fetkovich[35] in his Figs. 2A and B. The type curves corresponding to ω = 0.001 and λ =1E-6 are shown in **Fig. 9** for a range of r_{eD} from 100 to 150,000.

In this case, the constant flow rate period is shown for large values of the r_{eD}.

Once ω and η_{mD} are known, a type curve can be used to compute production rates for a particular reservoir.

A type curve match should provide information about the fracture permeability, k_{fb} and total storativity, $(\phi c_t)_t$.

The production rate as a function of time may be graphed on tracing paper, and then placed over the desired type curve. From a match point, the bulk fracture permeability, may be obtained from the dimensionless-real flow rate match:

$$k_{fb} = \frac{141.2\mu B}{h\left[p_i - p_{wf}\right]}\left(\frac{q(t)}{q_D(t_D)}\right)_M \qquad (35)$$

Similarly, from the dimensionless-real time match point, the total storativity may be obtained:

$$(\phi c_t)_t = \phi_m c_{tm} + \phi_{fb} c_{tf} = \frac{2.637\,x10^{-4} k_{fb}}{\mu r_w^{\,2}}\left(\frac{t}{t_D}\right)_M \qquad (36)$$

In a similar manner, using the definition of dimensionless fracture storage, the fracture storativity can be obtained:

$$\phi_{fb} c_{tfb} = \left[\ \phi_m c_{tm} + \phi_{fb} c_{tf}\ \right]\omega \qquad (37)$$

In addition, because ω and λ were determined by selection of the type-curve, information about the matrix block geometry and dimensions can be obtained, as indicated by the shape factor α, if k_m can be obtained from core analysis. Using the following equation (equaling lamda of definitions):

$$\alpha = \frac{C_{fbD}\,\eta_{mD}\,k_{fb}}{S_f\,k_m\,r_w^{\,2}} \qquad (38)$$

where the characteristic dimension is:

$$\varsigma = \sqrt{\frac{4n\left[n+2\right]}{\alpha}} \qquad (39)$$

Type–curve matching example

The production decline field data for an oil reservoir is shown in in Table 1. The production rate as a function of time was graphed on tracing paper and placed over the type curve corresponding to $\omega = 0.001$, $\eta_{mD} = 10^{-6}$, $S_f = 6$ and $r_{eD} = 5000$ generated with Cinco-Ley et al. model (see **Fig. 10**). The fracture permeability, k_{fb}, can be calculated from the the dimensionless-real flow rate match point, using data in Table 1 and Eq. 35:

$$k_{fb} = \frac{141.2(1)1}{480\left[11500 - 5000\right]}\left(\frac{5000}{0.015}\right) = 15 \quad mD$$

Similarly, from the real-dimensionless time match and using Eq. 36, the total storativity is obtained:

$$\phi_m c_{tm} + \phi_{fb} c_{tf} = \frac{2.637\,x10^{-4}(15)}{(1)(0.25)^2}\left(\frac{24}{150000}\right) = 10^{-5} \quad psi^{-1}$$

The product for the fracture:

$$\phi_{fb} c_{tfb} = 10^{-5}\,x10^{-3} = 10^{-8}\ psi^{-1}$$

for cubic blocks:

$$C_{fbD} = \frac{C_{fb} V_b \varsigma}{V_m} = \frac{A_{surf} V_b \varsigma}{V_b V_m} = \frac{6H^2}{H^3} H = 6$$

The interporosity flow shape factor is:

$$\alpha = \frac{6(10^{-2})15}{6(1)(0.25)^2} = 0.24\ ft^{-2}$$

The size of matrix blocks is:

$$\varsigma = \sqrt{12/0.24} = 7.07\ ft$$

CONCLUSIONS

The main purpose of this work has been to present a more general decline curve analysis for NFR based on the transient interporosity flow, including the fracture skin effect.

From the results of this study, the following conclusions can be established:

1. The model permits an easy change of the matrix block geometry.
2. Approximate analytical solutions for short and long times are presented; others previously presented solutions are particular cases (Chen et al.[29]).
3. For decline curve analysis, the use of the Warren and Root Model for the decline analysis of double porosity systems can be justified by using a matrix-fracture flow restriction.
4. The fracture skin can be confirmed by other sources, such as that from thin section of cores.
5. The bulk fracture parameters of permeability and the storativity and the outer radius can be estimated through the methodology of this study.
6. The estimated outer radius considering transient matrix to fractures transfer obtained in this work is higher than the value of pseudosteady state given by Da Prat et. al.[1]

NOMENCLATURE

A = drainage area, ft^2.

B = formation volume factor, RB/STB.

c_t = compressibility, psi^{-1}.

C_A = dimensionless pseudo steady state shape factor.

C_{fb} = fracture area; is the ratio between matrix surface and rock volume, ft^{-1}.

h = formation thickness, ft.
H = matrix block size, ft.
In = modified Bessel function, first kind, nth order.
k = permeability, mD.
Kn = modified Bessel function, second kind, nth order.
p = pressure, psi.
$\overline{p}$ = Laplace transform of p .
p_{wf} = wellbore flowing pressure, psi.
$q(t)$ = volumetric rate, bbl/day.
N_p = cumulative production, bbl.
n = number of normal set of fractures.
r_D = dimensionless radius.
r_e = outer boundary radius, ft.
r_{eD}' = effective dimensionless well outer boundary radius.
r_w' = wellbore radius, ft.
r_w' = effective wellbore radius, ft.
s = Laplace space parameter.
S_f = fracture skin.
S_w = van Everdingen and Hurst skin factor.
t = time, hours.
t_{DA} = dimensionless time based on drainage area A.
V = ratio of total volume of medium to bulk volume.
x = thickness, ft.
α = interporosity flow shape factor, ft^{-2}.
ς = characteristic dimension of the heterogeneous medium, ft.
λ = dimensionless matrix-fracture permeability ratio, reflects the intensity of the fluid transfer matrix-fractures.
η = diffusivity.
μ = viscosity, cp.
ϕ = porosity, fraction.
ω = dimensionless fracture storativity, is the ratio of the storage capacity of the fracture to the total capacity of the medium.

Subscripts

b = bulk (matrix and fractures).
D = dimensionless.
d = damaged zone.
e = external.
f = fracture
m = matrix
surf = matrix-fracture surface
t = total

ACKNOWLEDGMENTS

Our appreciation to Eng. Guadalupe Galicia for her careful and constructive reviews. Discussions with Eng. Guillermo Bernal and M.Sc. Geophysist Arturo Castro were invaluable. Special thanks to Claudia Mollinedo and the late Geologist Cesar Rosas for their assistance in the field. Portion of this study were done by M. Sc. Hector Pulido as graduate degree requirements. Financial support was provided by PEMEX.

REFERENCES

1. Da Prat, G., Cinco-Ley, H. and Ramey, H. J. Jr., 1981: *Decline Curve Analysis Using Type Curves for Two Porosity System*, SPEJ (June), 354-362.
2. Kucuk, F. and Ayestaran, L., 1983*: Analysis of Simultaneously Measured Pressure and Sandface Flow Rate in Transient Well Testing,* paper SPE 12177 presented at the Annual Technical Conference and Exhibition, San Francisco, CA. Oct. 5-8.
3. Stewart, G., Meunier D. and Wittman, M. J., 1983: *Afterflow Measurement and Doconvolution in Well Analysis,* paper SPE 12174 presented at the Annual Technical Conference and Exhibition, San Francisco, CA. Oct. 5-8.
4. Pirson, J. S., 1953: *Performance of Fractured Oil Reservoirs*, Bull., AAPG, vol. 37, 232-244.
5. Pollard, P., 1959: *Evaluation of Acid Treatments from Pressure Build-up Analysis*, Trans., AIME 216, 38-43.
6. Barenblantt, G. I. and Zheltov, Iu., 1960: *Fundamental Equations of Filtration of Homogeneous Liquids in Fissured Rocks* (in Russian), Soviet Physics Doklady, vol 5, 522-525.
7. Barenblatt, G. I., Zheltov, Iu. P. and Kochina, I. N., 1960: *Basic Concepts in the Theory of Seepage of Homogeneous Liquids in Fissured Rocks, Journal* Applied Mathematical and Mechanics, 24 (5), pp. 1286-1303.
8. Warren, J. E. and Root, P. J., 1963: *The Behavior of Naturally Fractured Reservoirs, Soc. Pet. Eng. J.*(Sep.), Vol. 3, 245-255; *Trans*. AIME, 228.
9. Warren, J. E. and Root, P. J., 1965: *Discussion of Unsteady State Behavior of Naturally Fractured Reservoirs, Soc. Pet. Eng. J. (March) 64-65, Trans*., AIME, 228, 245-255.
10. Odeh, A. S., 1965: *Unsteady - State Behavior of Naturally Fractured Reservoirs, Soc. Pet. Eng. J.* (March) 60-66, *Trans*. AIME, 234.
11. Adams, A. R., Ramey, H. J., Jr. and Burguess, R. J., 1968: *Gas Well Testing in a Fractured Carbonate Reservoir*, JPT (Oct.) 1187-1194; Trans., AIME 243.
12. Kazemi, H., 1969: *Pressure Transient Analysis of Naturally Fractured Reservoirs with Uniform Fracture Distribution, Soc. Pet. Eng. J*. (Dec.), 451-462; *Trans.* AIME, 246.
13. Gringarten, A. C. and Witherspoon, P. A., 1972: *A Method of Analyzing Pumping Test Data from*

Fractured Aquifer, Proc. Symp. Percolation Fissured Rock, Int. Soc. Rock Mech., Stuttgart T3, b-1-b9.

14. de Swaan, O. A., 1975: *Analytical Solutions for Determining Naturally Fractured Reservoir Properties by Well Testing*paper SPE 5346 presented at the SPE 45th Annual California Regional Meeting in Ventura, April 2-4, SPEJ (June, 1976, 117-122); *Trans.* AIME 261.
15. Crawford, G. E, Hagedorn, A. R. and Pierce, A. E., 1976: *Analysis of Pressure Buildup Tests in a Naturally Fractured Reservoir, J. Pet. Tech*. (Nov.) 1295-1300.
16. Strobel, C. J, Gulati, M. S. and Ramey, H. J. Jr. 1976: *Reservoir Limit Tests in a Naturally Fractured Reservoir- A Field Case Study Using Type Curves*, *J*. Pet. Tech. (Sep.) 1097-1106.
17. Mavor, M. L. and Cinco Ley, H., 1979: *Transient Pressure Behavior of Naturally Fractured Reservoirs,* paper SPE 7977 presented at the Calif. Regional Meeting, Ventura, Ca., April 18-20.
18. Streltsova, T. D., 1976: *Hydrodynamics of Groundwater Flow in Fractured Formations*, Water Res. Research (June), vol. 12, No. 3, 405-414.
19. Najurieta, H. L., 1980: *A Theory for Pressure Transient Analysis in Naturally Fractured Reservoir, J. Pet. Tech* (July), 1241- 1250.
20. Kucuk, F. and Sawyer, W. K., 1980: *Transient Flow in Naturally Fractured Reservoirs and its Application to Devonian Gas Shales*, paper SPE 9397, presented at the 55th Annual Fall Technical Conference and Exh. in Dallas, Tex, (Sep 21-24).
21. Gringarten, A., C., 1979: *Flow Tests Evaluation of Fractured Formations,* paper presented at the symposium on "Recent Trends in Hydrogeology". Berkeley, CA, Feb. 8-9.
22. Da Prat, G., Ramey, H. J., Jr. and Cinco-Ley, H., 1981: *A Method to Determine the Permeability-Thickness Product for a Naturally Fractured Reservoirs,* paper SPE 9906 presented at California Regional Meeting, Bakersfield, CA. March 25-26.
23. Bourdet, D. and Gringarten, A. C., 1980: *Determination of Fissure Volume and Block Size in Fractured Reservoirs by Type Curve Analysis*, paper SPE 9293 presented at the 55th Annual Technical Conference and Exhibition, Dallas, Tex., Sep. 21-24.
24. Gringarten, A. C., Burgess, T. M., Viturat, D., Pelisser, J. and Aubry, M., 1981: *Evaluating Fissured Formation Geometry from Well Test Data: A Field Example*, paper SPE 10182 presented at the 56th Annual Technical Conference and Exhibition, San Antonio, Texas, Oct. 5-7..
25. Gringarten, A. C., 1982: *Interpretation of Tests in Fissured Reservoirs and Multilayered with Double Porosity Behavior: Theory and Practice,* paper SPE 10044, presented at International Petroleum Exhibition and Technical Symposium, Beijing, China, March 26-28.
26. Cinco Ley, H. and Samaniego, V. F., 1982: *Pressure Transient Analysis for Naturally Fractured Reservoirs,* paper SPE 11026. presented at the 57th Annual Fall Technical Conference and Exhibition New Orleans, La., September 26-29.
27. Streltsova, T. D., A., 1982: *Well Pressure Behavior of Naturally Fractured Reservoirs,* paper SPE 10782, presented at the California Regional Meeting, San Francisco, Ca., March 24-26.
28. Serra, K., Reynolds, A. C. and Raghavan, R., 1982: *New Pressure Transient Analysis Methods for Naturally Fractured Reservoirs,* paper 10780 presented at the California Regional Meeting, Bakersfield, Ca., March 27-29. *J. Pet. Tech*. (Dec.1983) 2271-2284.
29. Chen, C. C., Serra, K., Reynolds, A. C. and Raghavan, R., 1985: *Pressure Transient Analysis Methods for Bounded Naturally Fractured Reservoirs*, SPEJ (June), 451-464.
30. Moench, A. F. and Ogata, A., 1984: *A Double Porosity Model for a Fissured Groundwater Reservoir with Fracture Skin*, Water Resources Research, vol. 20, No. 7, 831-846.
31. Cinco Ley H., Samaniego, V. F and Kucuk, F., 1985: *The Pressure Transient Behavior for a Naturally Fractured Reservoirs with Multiple Block Size*, paper SPE 14168 presented at the Annual Technical Conference and Exhibition, Bakersfield, CA., March 27-29.
32. van Everdingen, A. F. and Hurst,W., 1949: *The Application of the Laplace Transform to Flow Problems in Reservoirs, Trans.*, AIME 186, 305-324.
33. Stehfest, H., 1970: *Algorithm 368: Numerical Inversion of Laplace Transforms, Communications of the ACM* (Jan.) 13, 47-49.
34. Jacob, C. E. and Lohman, S. W., 1952: *Nonsteady Flow to a Well of Constant Drawdown in an Extensive Aquifer,* Trans. Am. Geophys. Union (August) 559-569.
35. Fetkovich, M. J., 1980*: Decline Curve Analysis Using Type Curves*, J. Pet. Tech. (June), 1065-1077.
36. Tsarevich, K. A. and Kuranov, I. F., 1956: *Calculation of the flow Rates for the Center Well in a Circular Reservoir Under Elastic Conditions,* Problems of Reservoir Hydrodynamics, Leningrad, Part. 1, 9-34.
37. Sageev, A., Da Prat, G. and Ramey, H. J., 1985: *Decline Curve Analysis for Double Porosity Systems,* paper SPE 13630 presented at the Annual Technical Conference and Exhibition, Bakersfield, CA., March 27-29.
38. Ehlig- Economides, C. A., 1979: *Well Test Analysis for Wells Produced at a Constant Pressure,* Ph. D dissertation, Stanford, University Stanford, Calif.

39. Uldrich, D. O. and Ershaghi, I., 1978: *A Method for Estimating the Interporosity Flow Parameter in Naturally Fractured Reservoirs*, paper SPE 7142 presented at the California Regional Meeting, San Francisco, April 12-14. *Soc. Pet. Eng. J. (Oct.1979)* 324-332.

Tabla 1. Data used in field problem.

T (days)	Q (bbl/day)	T (days)	Q (bbl/day)
100	10150	2700	3872
300	9690	3400	3517
400	8850	4000	3314
600	8175	5000	2767
800	7425	7000	2405
1200	6486	9000	2270
1700	5475	12000	2270
2100	4378	20000	2198

$P_i = 11500\ psi, P_{wf} = 5000\ psi, S_w = -4.09, h = 480\ ft,$

$\mu = 1\ cp\ ,\ B = 1\ RB\ /\ STB\ ,\ r_w = 0.25\ ft\ ,\ \omega = 0.001$

$\lambda = 10^{-6}\ ,\ r_e = 1500\ ft\ ,\ r_{eD}' = 100\ ,\ r_w' = 15\ ft\ .$

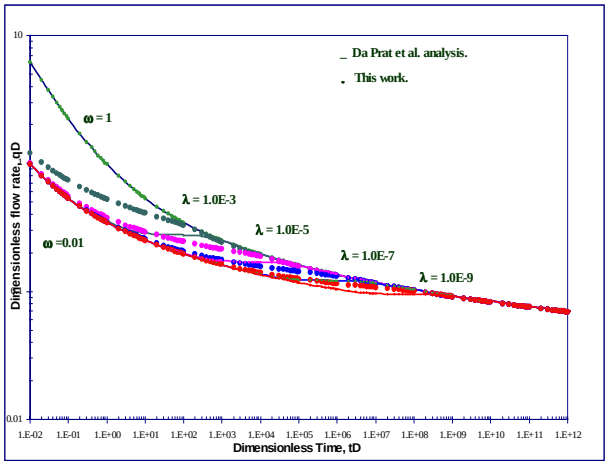

Fig. 1. Log-log dimensionless flow rate behavior for constant pressure production conditions, infinite naturally fractured reservoir, S_f =0, S_w=0.

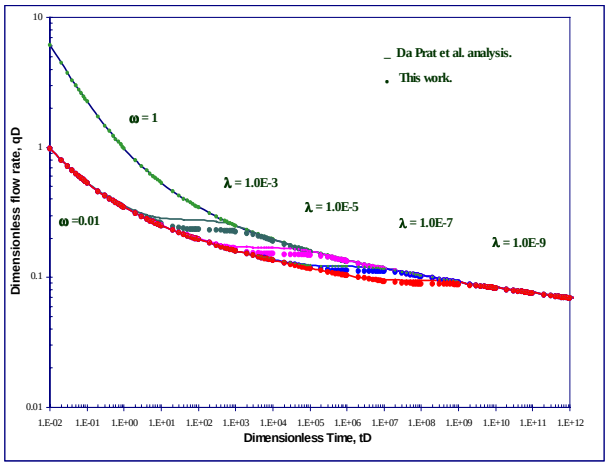

Fig. 2. Log-log dimensionless flow rate behavior for constant pressure production conditions, infinite naturally fractured reservoir, S_f = 6, S_w=0.

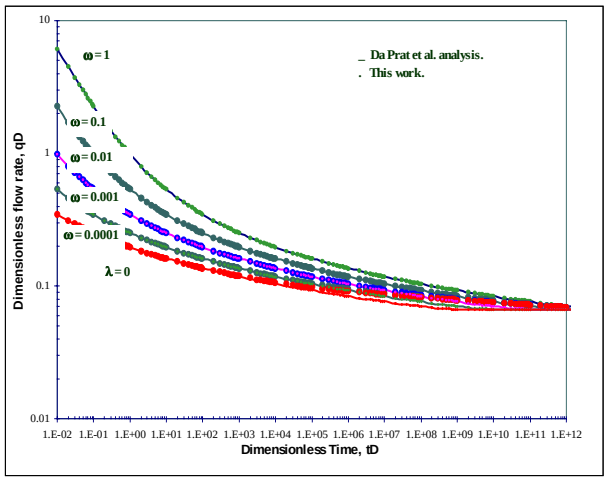

Fig. 3. Log-log dimensionless flow rate behavior for constant pressure production conditions, infinite naturally fractured reservoir, k_m = 0, S_f = 0, S_w=0.

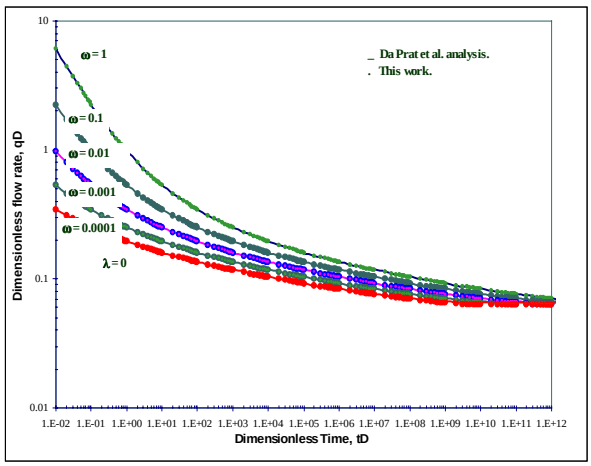

Fig. 4. Log-log dimensionless flow rate behavior for constant pressure production conditions, infinite naturally fractured reservoir, k_m = 0, S_f = 6, S_w=0.

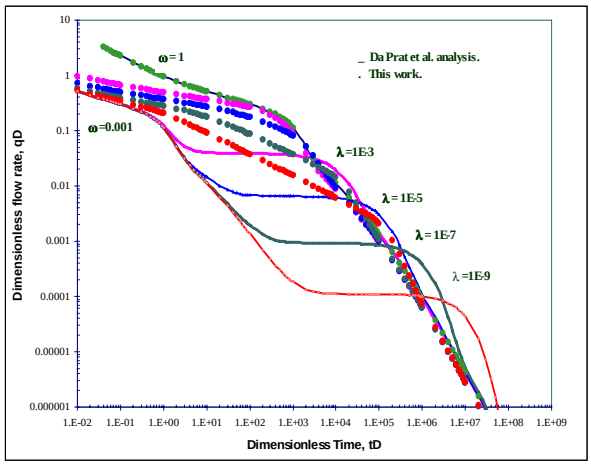

Fig. 5. Log-log dimensionless flow rate behavior for constant pressure production conditions in a bounded naturally fractured reservoir, r_{eD} = 50, S_f =0, S_w=0.

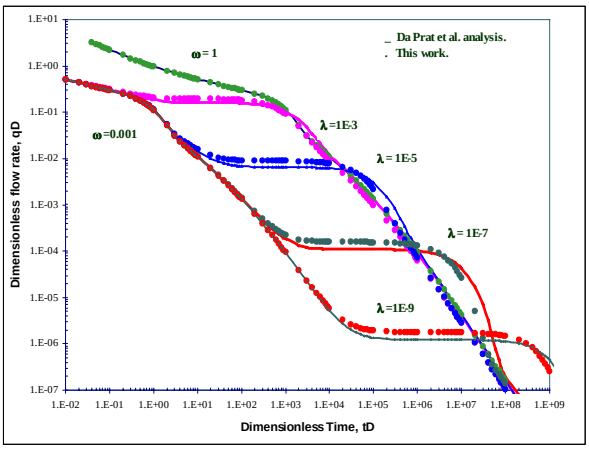

Fig.6. Log-log dimensionless flow rate behavior for constant pressure production conditions in a bounded naturally fractured reservoir, r_{eD}=50, S_f =6, S_w=0.

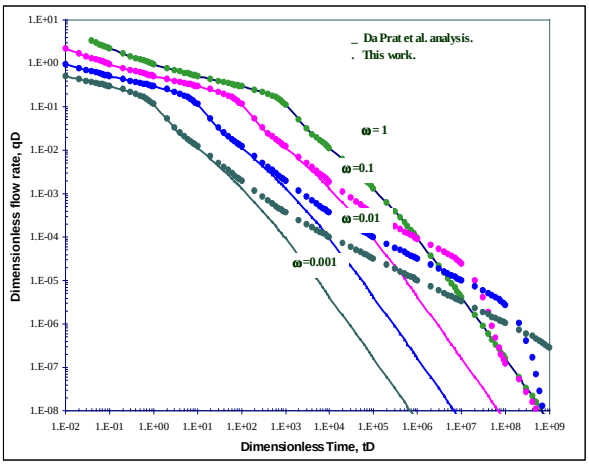

Fig. 7. Log-log dimensionless flow rate behavior for constant pressure production conditions in a bounded naturally fractured reservoir, the reserves are located only in the fractures, r_{eD}=50, S_f =0, S_w=0.

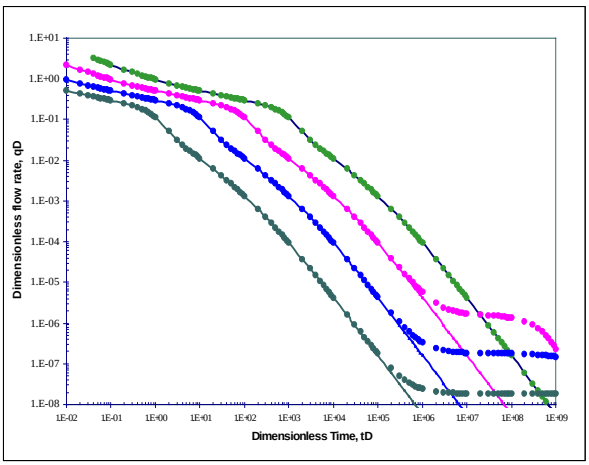

Fig. 8. Log-log dimensionless flow rate behavior for constant pressure production conditions in a bounded naturally fractured reservoir, the reserves are located only in the fractures, r_{eD} =50, S_f =6, S_w=0.

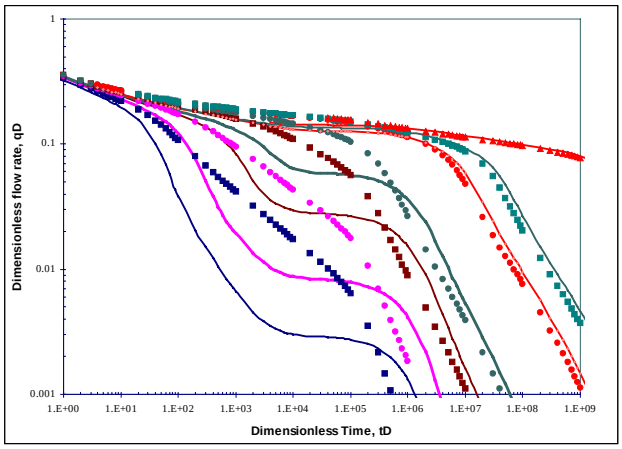

Fig. 9. Type curves used for decline curve analysis in NFR for reD: 100, 200, 500, 1,000, 5000, 10,000, 150,000, S_f =0, S_w=0.

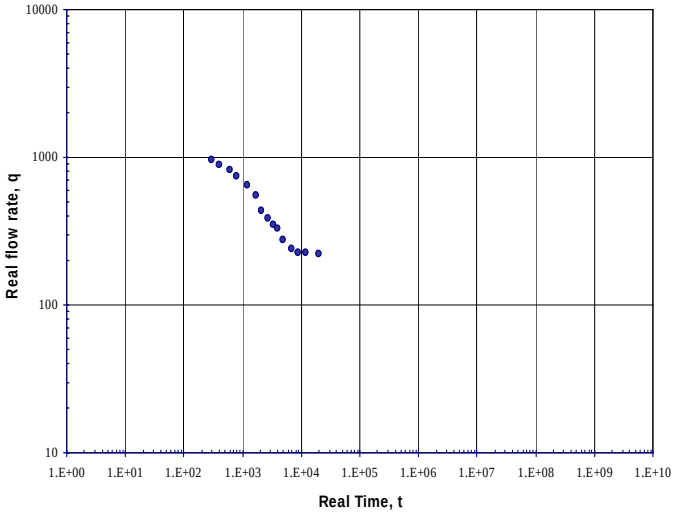

Fig. 10. Type-curve matching example.